Inelastic Response of Structures 16

Abstract

The conventional design approach works with factored loads and reduced material capacities such as strength. When subjected to service loads, the structure is detailed such that it behaves elastically. For extreme loadings, the structure is allowed to experience a limited amount of deformation beyond the elastic limit. This deformation is called "inelastic" since in contrast to elastic deformation, when the loading is removed, the structure does not return to its original position. Up to this point in the text, we have assumed the behavior to be elastic. In Chap. 10, we included geometric nonlinear effects but still assumed elastic behavior. Here, we introduce an additional effect, inelastic behavior. We start with an in-depth discussion of the stress–strain behavior of structural steels and concrete, apply these ideas to beams subjected to inelastic bending, and then develop an analysis procedure to determine the inelastic response of frame-type structures. This approach allows one to estimate the "maximum" loading that a structure can support, i.e., the "limit load." Examples illustrating the influence of inelastic behavior on the ultimate capacity are included.

16.1 Stress–Strain Behavior of Structural Steels

Steel and concrete are the two most popular construction materials. Steels with low carbon content are usually referred to as "structural" steels since they are used primarily to fabricate structural elements such as W, T, and I shapes. Structural steels have desirable properties such as strength, uniformity, weldablity, and ductility. The latter property is related to the ability of structural steels to experience significant deformation prior to fracture.

Figure 16.1 shows a typical stress–strain plot for a mild (low carbon) steel. There are four distinct deformation zones: elastic; yielding; strain hardening; and necking. The stress remains constant as the specimen yields until the strain, ε_y', is reached. Beyond this level, strain hardening occurs with the stress increasing to its "ultimate" value and then decreasing to the value at which rupture occurs. The yield zone for mild steel is relatively large, on the order of 20 times the yield strain ε_y. Another

J.J. Connor, S. Faraji, *Fundamentals of Structural Engineering*,
DOI 10.1007/978-3-319-24331-3_16

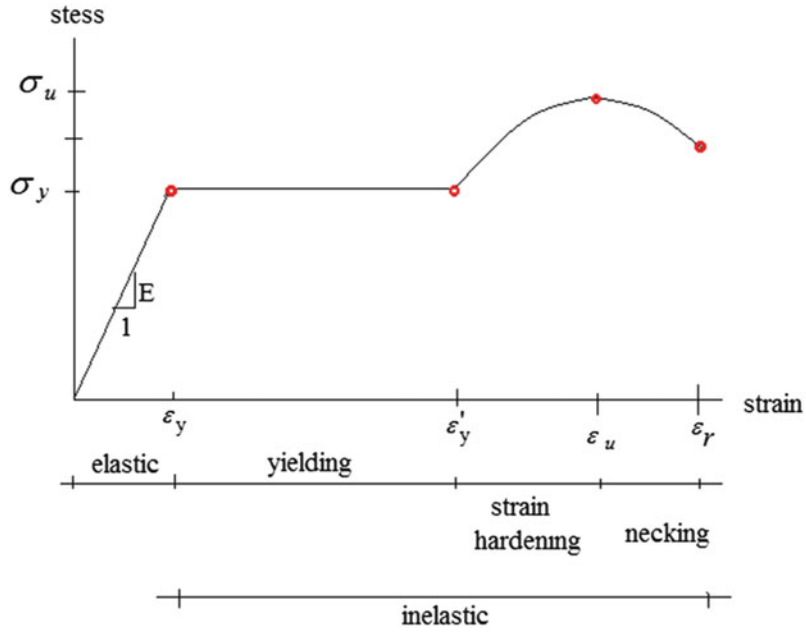

Fig. 16.1 Typical stress–strain curve for mild structural steel

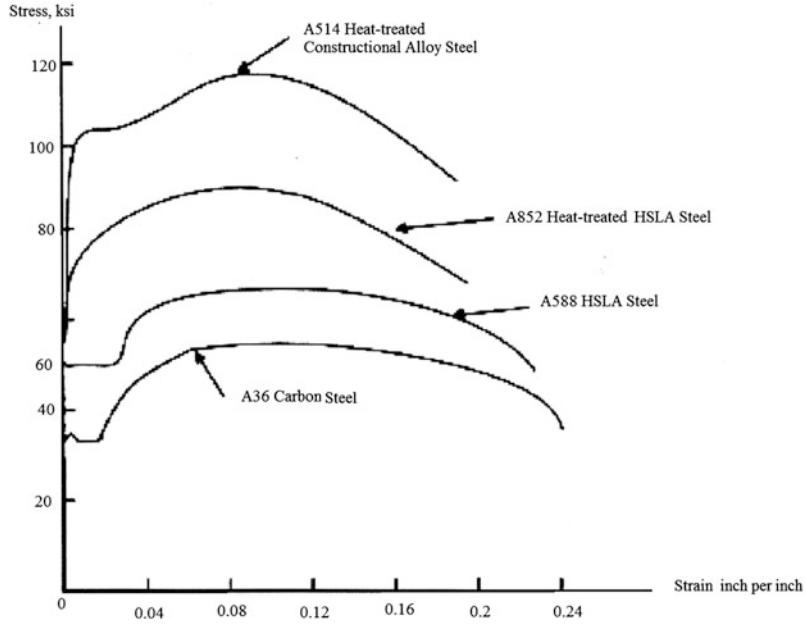

Fig. 16.2 Steel properties—structural steels

measure is the rupture strain ε_r. By definition, ε_r is the fractional change in length of the specimen and is usually expressed as a percentage. For mild steel, the percent elongation is about 24 %. Ductility refers to the ability to deform plastically without fracturing and is measured by the ratio $\frac{\varepsilon_r}{\varepsilon_y}$. This ratio is large compared to 1. The last measure of interest is the toughness, defined as the energy required to fracture the material. Toughness is equal to the area under the stress–strain curve to fracture, and is usually expressed as a multiple of R, the area under the linear portion of the stress–strain curve.

Figure 16.2 lists the stress–strain plots for a range of common structural steels. Note that as the yield stress and the ultimate stress increase, the yield zone and the rupture strains decrease. There is a

trade-off between ductility and strength. The yield zones for the two lower strength steels are essentially equal $\left(\frac{\varepsilon_y'}{\varepsilon_y} \approx 13\right)$ whereas the higher strength steels shift directly from elastic behavior into strain hardening.

16.2 Inelastic Moment–Curvature Relationships

The fact that structural steels can experience significant deformation before rupturing is the basis for developing an analysis procedure for tracking the response as the structure passes from the elastic range through the yielding zone up to rupture. The starting point for the analysis is establishing the moment capacity of a beam subjected to inelastic bending.

Assuming a cross section remains a plane, the extensional strain varies linearly with distance from the centroidal axis.

$$\varepsilon = y\chi \tag{16.1}$$

where χ is the curvature of the centroidal axis. Given χ, one computes ε and then determines the stress using a nonlinear stress–strain relation such as shown in Fig. 16.1.

$$\varepsilon \rightarrow \sigma = f(\varepsilon) \rightarrow \sigma = f(\chi) \tag{16.2}$$

The moment is defined by the following integral,

$$M = \int_A (-y)\sigma \mathrm{d}A = M(\chi) \tag{16.3}$$

This integral is usually evaluated numerically; one ranges over χ and constructs a plot of M vs. χ. The exact form depends upon the assumed stress–strain relationship and the shape of the cross section.

In order to obtain an analytical solution, the stress–strain curve is usually approximated with a linear model. The simplest model for steel is based on the assumption of elastic perfectly plastic fracture behavior; the increase in stress due to strain hardening is neglected. Figure 16.3 illustrates this behavior.

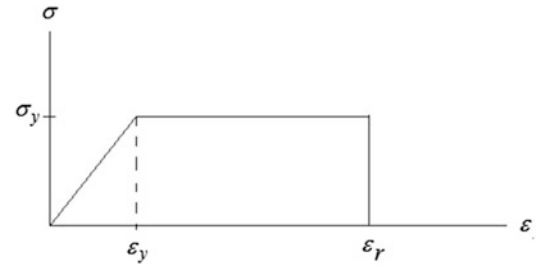

Fig. 16.3 Elastic perfectly plastic fracture (EPPF) model

Using this model, and applying (16.1)–(16.3) to a rectangular cross section, one obtains the plot shown in Fig. 16.4.

$$M_{\mathrm{y}} = \sigma_{\mathrm{y}}\left(\frac{bh^2}{6}\right)$$

$$M_{\mathrm{r}} = \frac{3}{2}M_{\mathrm{y}}\left\{1 - \frac{1}{3}\left(\frac{\varepsilon_{\mathrm{y}}}{\varepsilon_{\mathrm{r}}}\right)^2\right\}$$

$$\chi_{\mathrm{y}} = \frac{2\varepsilon_{\mathrm{y}}}{h} \quad \chi_{\mathrm{r}} = \frac{2\varepsilon_{\mathrm{r}}}{h}$$

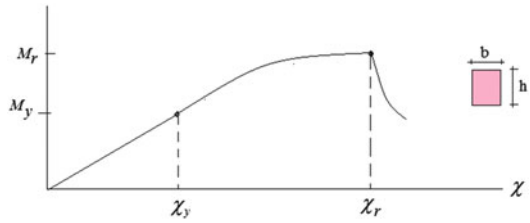

Fig. 16.4 Moment–curvature plot—rectangular sector and EPPF material

The outer fiber fractures at $\chi = \chi_{\mathrm{r}}$, resulting in a discontinuity in the derivative.
For $\chi > \chi_{\mathrm{r}}$, yielding progresses over the section and the moment capacity rapidly decreases.

Wide flange sections behave differently since the moment is carried primarily by the flanges. Fracture in the flanges results in a significant loss of moment capacity, especially when the sections are thin-walled since, in this case, the fracture occurs simultaneously throughout the flange thickness. A typical plot is shown in Fig. 16.5.

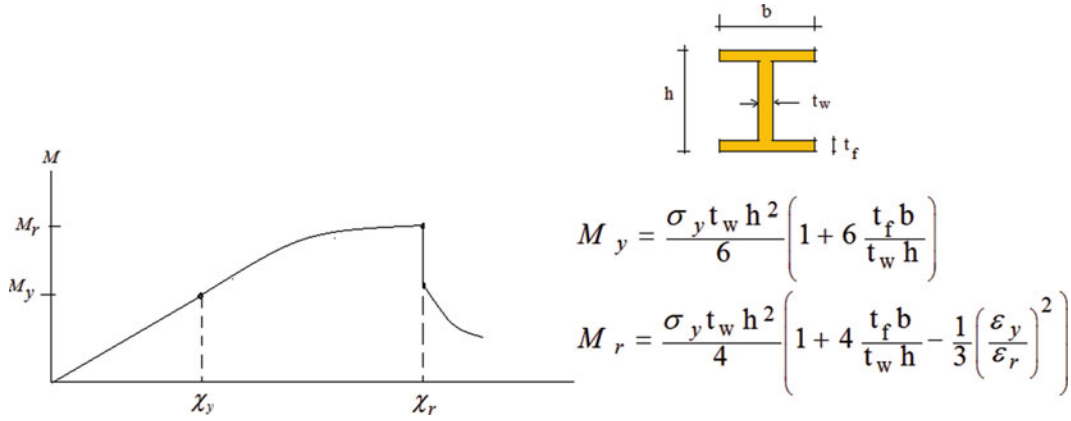

Fig. 16.5 Moment–curvature plot—thin walled wide flange section and EPPF material

From a computer implementation perspective, it is convenient to represent the moment–curvature relations with the bilinear approximation shown in Fig. 16.6. Nonlinear analysis is required to evaluate the load-deflection behavior. With this type of approximation, when yielding occurs, one replaces the elastic stiffness with a "linearized" tangent stiffness. The simplest possible strategy is to

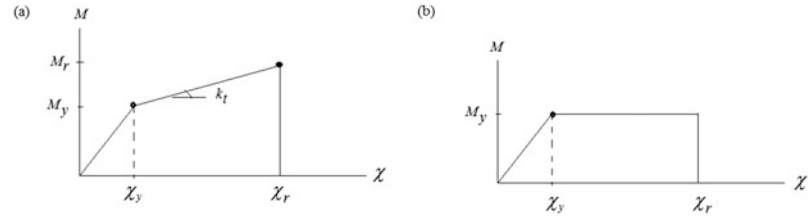

Fig. 16.6 Bilinear moment–curvature models. (**a**) General bilinear model and (**b**) EPPF model

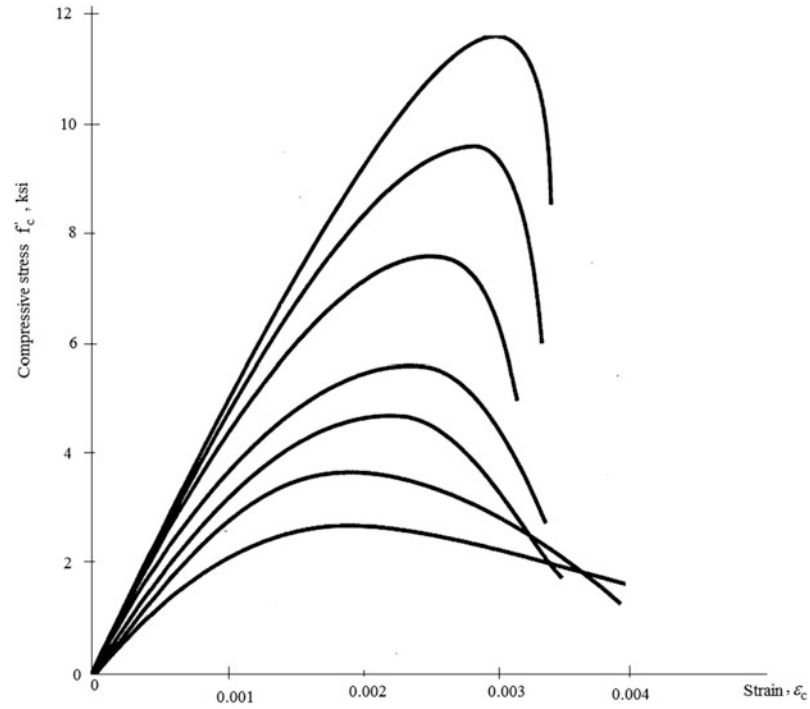

Fig. 16.7 Compressive stress–strain curves for concrete

work with an elastic perfectly plastic fracture model, i.e., to assume the tangent stiffness is negligible for $\chi_y < \chi < \chi_r$. This behavior is introduced by inserting a hinge at the location of the cross section and applying a constant moment equal to M_y. When $\chi \geq \chi_r$, the constant moment is removed, resulting in no moment capacity at the section.

Although the discussion has been focused on steel, the concept of a bilinear moment–curvature model is also adopted for concrete. The behavior of concrete differs from that of steel in that the stress–strain relationship for concrete exhibits strain softening (a reduction in stress beyond the peak value with increasing strain) and the peak strain is several order of magnitude smaller than that of steel. Typical plots are shown in Fig. 16.7. The limiting strain, ε_r, corresponds to crushing of the concrete and is of the order of 0.0004.

Assuming the strain varies linearly over the cross section; one can construct the moment–curvature relationship. A typical plot for an under-reinforced section is shown in Fig. 16.8. For computer-based analysis, one uses the nonlinear form. For hand computation, this form is approximated with an elastic perfectly plastic fracture model where M_y' is considered to be the ultimate moment capacity. A detailed discussion of this topic is contained in Winter and Nilson [1].

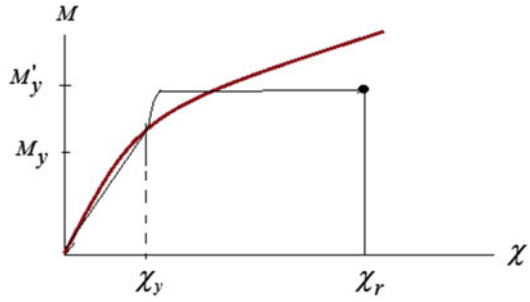

Fig. 16.8 Moment–curvature relationship—concrete beams

16.3 Limit Analysis: A Simplified Approach

Given the properties of a structure and a particular loading distribution, it is of interest to establish the peak magnitude of the loading that the structure can support, i.e., the limit of the loading. In what follows, we describe a procedure based on using an elastic perfectly plastic fracture model. Starting at a low load level, one carries out an elastic analysis and identifies the section where the bending moment is a relative maximum. The loading is then scaled up such that the magnitude of the moment at that particular section equals its moment capacity. In this approach, the capacity is taken as the yield moment. At this loading limit, a hinge is inserted and a set of self-equilibrating concentrated moments equal to M_y are applied at the section. The modified structure is then examined with respect to its stability, i.e., its capacity to support additional load. If stable, the loading is increased until another cross section reaches its moment capacity. The structure is again checked for stability and, if stable, a hinge and the assumed set of moments are inserted. The process is continued until the modified structure is unstable. The following examples illustrate the limit analysis process.

Example 16.1

Given: A simply supported beam subjected to a uniform loading defined in Fig. E16.1a.

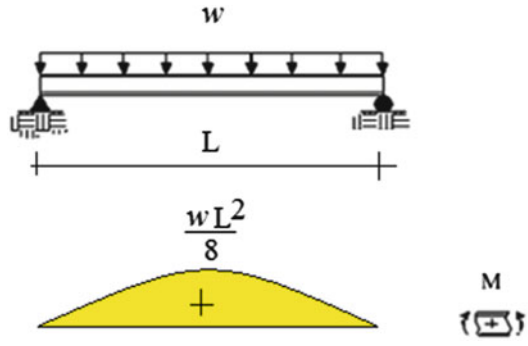

Fig. E16.1a

Determine: The load capacity.
Solution: The peak moment occurs at mid-span.

$$M_{\max} = \frac{wL^2}{8}$$

We increase the loading until $M_{\max} = M_y$.

$$M_y = \frac{w_1 L^2}{8}$$
$$\Downarrow$$
$$w_1 = \frac{8M_y}{L^2}$$

The modified structure for this load level is shown in Fig. E16.1b.

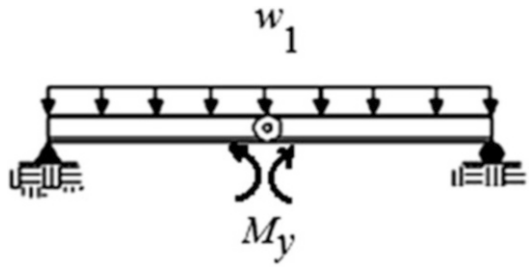

Fig. E16.1b

Any load increase will cause the structure to collapse downward since it has no capacity to carry any additional load. Therefore, $w_1 = w_{\max}$.

Example 16.2

Given: The fixed-ended beam subjected to a uniform loading defined in Fig. E16.2a.

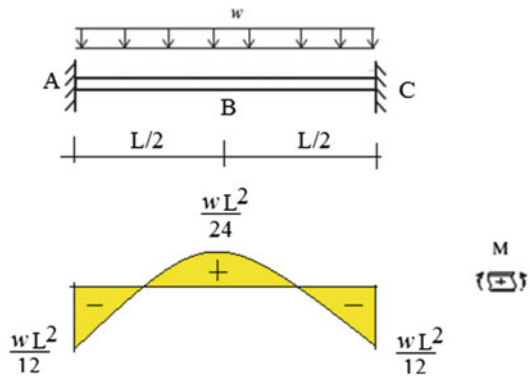

Fig. E16.2a

Determine: The load capacity.
Solution: The peak moment occurs at A and C. Therefore, yielding will first occur at these sections. We increase the loading until $M_{\max} = M_y$.

$$M_y = \frac{w_1 L^2}{12}$$
$$\Downarrow$$
$$w_1 = \frac{12 M_y}{L^2}$$

Inserting hinges at A and C results in a simply supported beam with end moments.

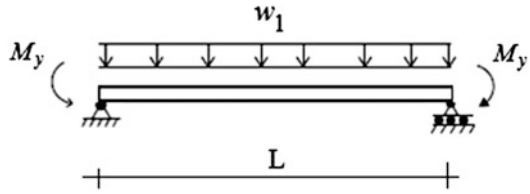

Fig. E16.2b

The next critical section is at mid-span. Applying an incremental load, Δw, increases the moment at mid-span.

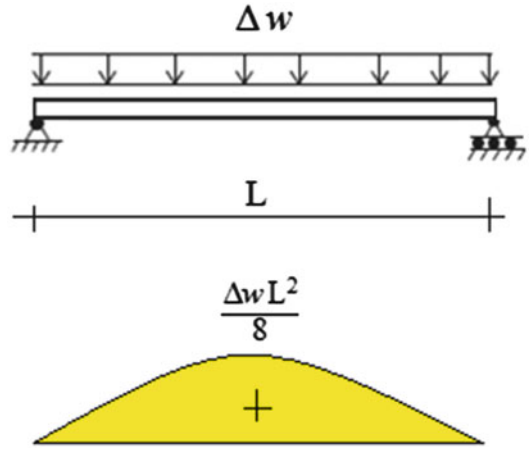

Fig. E16.2c

Then, superimposing the results for the two cases leads to the peak moment at mid-span which is set equal to M_y.

$$\frac{\Delta w L^2}{8} + \frac{w_1 L^2}{24} = M_y$$

Substituting for w_1,

$$\frac{\Delta w L^2}{8} = M_y - \frac{1}{2} M_y = \frac{1}{2} M_y$$

leads to

$$\Delta w = \frac{4}{L^2} M_y$$

Lastly,

$$w_{\max} = w_1 + \Delta w = \frac{16}{L^2} M_y$$

The final "limit state" is shown in Fig. E16.2d. This structure is unstable for any *additional transverse loading*.

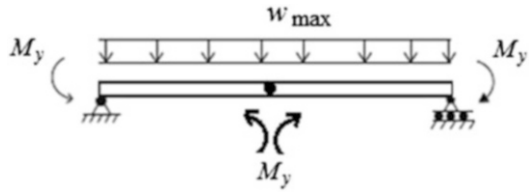

Fig. E16.2d

Example 16.3

Given: The two-span beam shown in Fig. E16.3a. Assume EI is constant.

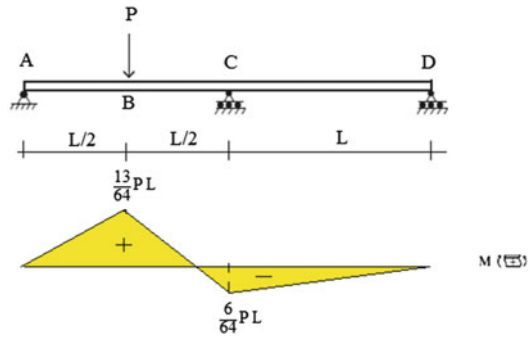

Fig. E16.3a

Determine: The limit state.
Solution: The moments at section B and C are relative maxima; the value at B is the largest, so yielding will occur first at this section.

$$M_B = \frac{13}{64} PL$$

$$M_C = -\frac{6}{64} PL$$

Load level 1:
We set M_B equal to M_y and insert a hinge at B.

$$\frac{13}{64} P_1 L = M_y$$

$$\Downarrow$$

$$P_1 = \frac{64}{13L} M_y$$

At this load level, the modified structure is

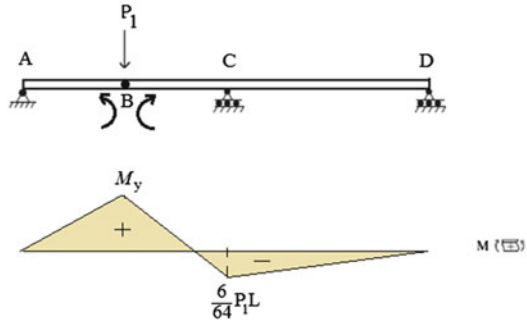

Fig. E16.3b

Load level 2:

We apply an incremental load, ΔP, to the modified structure leading to an incremental moment at C.

$$\Delta M_{\mathrm{C}} = \frac{L}{2}\Delta P$$

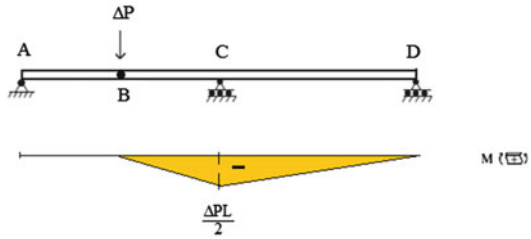

Fig. E16.3c

The total negative moment at C is

$$\left\{ M_{\mathrm{C}} = \frac{6}{64}P_1 L + \frac{\Delta P L}{2} \right\}$$

Setting $M_{\mathrm{C}} = M_{\mathrm{y}}$ leads to the limiting value for ΔP

$$\frac{6}{64}P_1 L + \Delta P \frac{L}{2} = M_{\mathrm{y}}$$

Substituting for P_1, one obtains

$$\Delta P = \frac{14}{13L}M_{\mathrm{y}}$$

Finally

$$P_{\max} = P_1 + \Delta P = \frac{78}{13L}M_{\mathrm{y}} = \frac{6}{L}M_{\mathrm{y}}$$

The limit state has hinges at B and C.

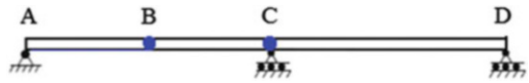

Fig. E16.3d

The procedure followed in the above examples involved applying the loading in increments and analyzing the structure at each load level. When yielding is reached at a particular load level, the structural stiffness is modified by inserting a hinge (i.e., zero rotational stiffness) at the yielded section. The loading process is continued until the structure becomes unstable. In general, instability occurs when the number of plastic hinges is equal to 1 plus the number of degrees of static indeterminacy. From a structural prospective, instability occurs when the tangent stiffness associated with the complete structure vanishes.

When evaluating the response, one must also check that the curvature at a yielded section does not exceed the "rupture" or "crushing" value. When this occurs, the moment capacity is set to zero. We did not carry out this computation in the above examples since it requires a computer-based procedure in order to obtain reliable results. Later in the chapter, we describe a computer procedure based on a finite element beam discretization combined with an incremental nonlinear solution strategy. Most modern structural software systems have this type of capability.

An alternative hand calculation approach to establishing the limit state is based on assuming a pattern of hinges that corresponds to a limit state and evaluating the corresponding load magnitude. One starts with the elastic moment diagram and identifies the sections where the moment is a relative maximum. At the limit state, the number of plastic hinges is equal to 1 plus the number of degrees of freedom. The load magnitude can be obtained either by applying the equilibrium equations or using the principal of virtual work which is an equivalent statement of equilibrium. The latter approach is generally more convenient. We illustrate this procedure with the following examples.

Example 16.4

Given: A two-span beam shown in Fig. E16.4a.

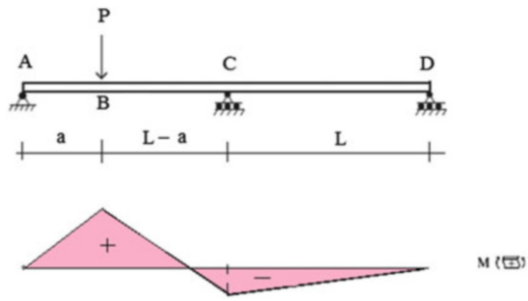

Fig. E16.4a

Determine: The limit state.
Solution: The critical state has two hinges. Noting the moment diagram, we locate them at Points B and C.

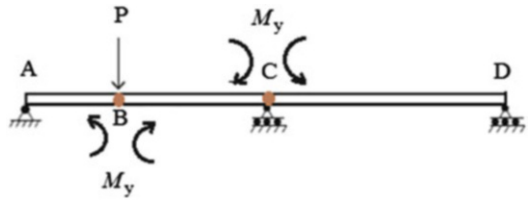

Fig. E16.4b

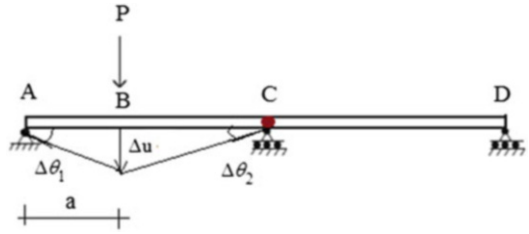

Fig. E16.4c

We use the principle of virtual work to establish the expression for P. Introducing a virtual displacement at B and evaluating the work done by P and the plastic moments lead to

$$P\Delta u - M_y(\Delta\theta_1 + \Delta\theta_2) - M_y\Delta\theta_2 = 0$$

The displacement terms are related by

$$\begin{cases} \Delta\theta_1 = \dfrac{\Delta u}{a} \\ \Delta\theta_2 = \dfrac{\Delta u}{L-a} \end{cases}$$

Substituting for the $\Delta\theta$ terms, the work equation reduces to

$$\Delta u\left\{P - \frac{M_y}{a} - 2M_y\left(\frac{1}{L-a}\right)\right\} = 0$$

This must be satisfied for arbitrary Δu. Then

$$P = M_y\left(\frac{1}{a} + \frac{2}{L-a}\right)$$

Example 16.5

Given: A two-story frame shown in Fig. E16.5a.

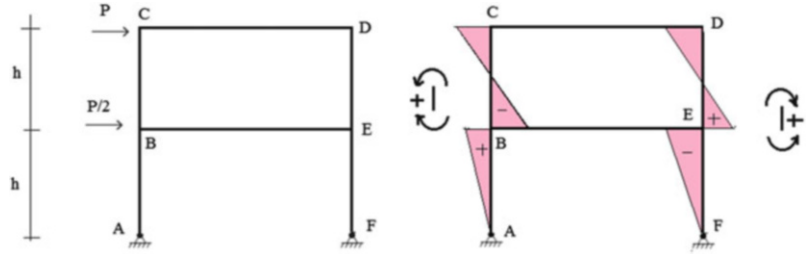

Fig. E16.5a

Determine: The limit state.

Solution: For this structure and loading, the relative moment maxima occur at the nodes. Therefore, plastic hinges will develop at the end of the members. When designing the members, most design codes require that one selects sectional properties such that yielding occurs only in the beams. We assume that condition is satisfied here, and work with the limit state shown below.

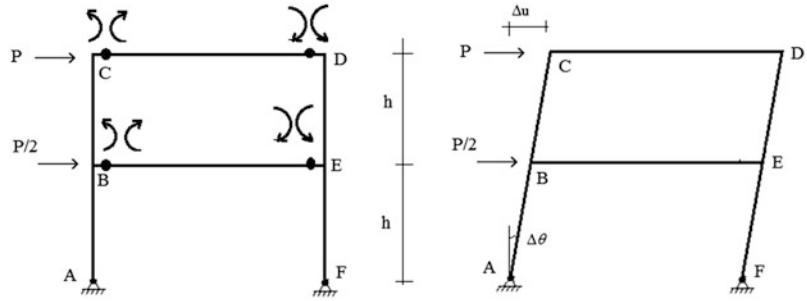

Fig. E16.5b

Introducing a virtual displacement at C, the work terms are

$$P\Delta u + \frac{P}{2}\frac{\Delta u}{2} - 4M_y\Delta\theta = 0$$

$$\Downarrow$$

$$\frac{5}{4}P\Delta u = 4M_y\Delta\theta = 4M_y\left(\frac{\Delta u}{2(h)}\right)$$

$$\Downarrow$$

$$P_{max} = \frac{8M_y}{5\ h}$$

In the above example, we assumed a particular plastic hinge pattern. Other patterns are also possible, each with a different limit load. One needs to examine *all possible patterns* in order to identify the minimum critical load. This operation is not feasible using hand computation for a complex structure. One needs to employ a computer-based nonlinear analysis scheme which generates the load displacement response allowing for the formation of plastic hinges up to the load level at which collapse is imminent. A particular nonlinear analysis scheme is described in the next section.

16.4 Nonlinear Analysis Scheme

We illustrate this method using the structure analyzed in Example 16.4. The first step involves discretizing the structure with a combination of elastic and plastic finite elements. A refined mesh is used in those zones where the moment is a relative maximum, such as adjacent to interior nodes and concentrated loads. Since the extent of plastic yielding is not known initially, one needs to iterate, starting with a single plastic element and adding additional plastic elements if necessary. This process is illustrated in Fig. 16.9.

The material behavior within a plastic segment is assumed to follow the bilinear moment–curvature model defined in Fig. 16.10. When $\chi < \chi_y$, the behavior is elastic, and the elastic stiffness k_E applies. When $\chi > \chi_y$, the behavior is inelastic and the reduced stiffness, k_t, is used. When $\chi > \chi_r$, the moment is set equal to zero, i.e., the section is considered to have no moment capacity.

The equilibrium equations for a member are generalized using the Principal of Virtual Displacements [2]. Consider the element shown in Fig. 16.11. Nodes are located at each end, and the nodal displacement measures are the translation and rotation.

Introducing matrix notation, these measures are expressed as

$$\underline{U}_1 = \begin{Bmatrix} v_1 \\ \theta_1 \end{Bmatrix} \quad \underline{U}_2 = \begin{Bmatrix} v_2 \\ \theta_2 \end{Bmatrix}$$

The transverse displacement is approximated as

$$v(x) = \underline{\Phi}_1 \, \underline{U}_1 + \underline{\Phi}_2 \, \underline{U}_2 \tag{16.4}$$

where $\underline{\Phi}_1$ and $\underline{\Phi}_2$ contain interpolation functions.

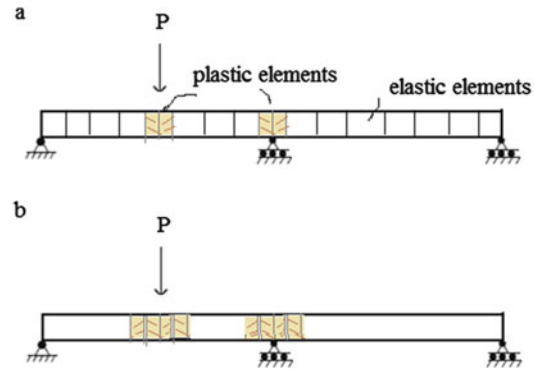

Fig. 16.9 Plastic element discretization. (**a**) Initial mesh and (**b**) expanded mesh

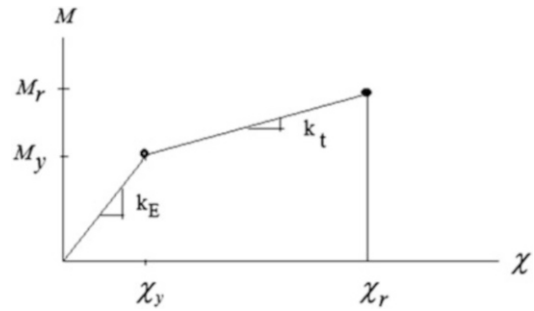

Fig. 16.10 Bilinear model

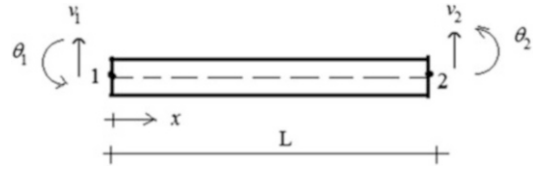

Fig. 16.11 Notation for end displacements

$$\begin{aligned}\underline{\Phi}_1 &= \left[1-3\left(\tfrac{x}{L}\right)^2+2\left(\tfrac{x}{L}\right)^3 \quad x-2\frac{x^2}{L}+\frac{x^3}{L^2}\right]\\ \underline{\Phi}_2 &= \left[3\left(\tfrac{x}{L}\right)^2-2\left(\tfrac{x}{L}\right)^3 \quad -\frac{x^2}{L}+\frac{x^3}{L^2}\right]\end{aligned} \tag{16.5}$$

Differentiating twice leads to the curvature

$$\begin{aligned}\chi = v_{,xx} &= \underline{\Phi}_{1,xx}\,\underline{U}_1 + \underline{\Phi}_{2,xx}\,\underline{U}_2\\ \underline{\Phi}_{1,xx} &= \left[-\frac{6}{L^2}+\frac{12x}{L^3} \qquad -\frac{4}{L}+\frac{6x}{L^2}\right]\\ \underline{\Phi}_{2,xx} &= \left[+\frac{6}{L^2}-\frac{12x}{L^3} \qquad -\frac{2}{L}+\frac{6x}{L^2}\right]\end{aligned} \tag{16.6}$$

Note that the curvature varies linearly over the segment in this approach. *Given the end displacements*, *one evaluates the curvature*, *and then the bending moment*.

The end forces are determined with the following virtual work requirement:

$$\int M\,\delta\chi\,\mathrm{d}x \;\equiv\; \underline{P}^{\mathrm{T}}{}_1\;\delta\underline{U}_1 + \underline{P}^{\mathrm{T}}{}_2\;\delta\underline{U}_2 \tag{16.7}$$

for arbitrary $\delta\underline{U}_1$ and $\delta\underline{U}_2$. Noting

$$\delta\chi = v_{,xx} = \underline{\Phi}_{1,xx}\;\delta\underline{U}_1 + \underline{\Phi}_{2,xx}\;\delta\underline{U}_2 \tag{16.8}$$

and expanding (16.7) result in

$$\begin{aligned}\underline{P}_1 &= \int \underline{\Phi}^{\mathrm{T}}{}_{1,xx}\,M\;dx\\ \underline{P}_2 &= \int \underline{\Phi}^{\mathrm{T}}{}_{2,xx}\,M\;dx\end{aligned} \tag{16.9}$$

When the behavior is inelastic, a numerical integration scheme, such as a 2 point Gaussian approximation, is used to evaluate the integrals. The moment is determined using Fig. 16.10.

Lastly, the global force equilibrium equation for the nodes is written as

$$\underline{P}_{\mathrm{E}} = \underline{P}_{\mathrm{I}} \tag{16.10}$$

where $\underline{P}_{\mathrm{E}}$ contains the external nodal loads and $\underline{P}_{\mathrm{I}}$ represents the nodal loads due to the member end actions which are functions of the nodal displacements. The solution scheme proceeds as follows. Suppose $U\big|_i$ represents the ith solution for the response due to P_{E_i}. The static error is

$$E\big|_i = P_{\mathrm{E}}\big|_i - P_{\mathrm{I}}\big|_i \tag{16.11}$$

We correct the error by introducing an incremental displacement $\Delta\underline{U}\big|_i$ which leads to the increment $\Delta\underline{P}_{\mathrm{I}}\big|_i$. The equilibrium requirement for $\Delta\underline{P}_{\mathrm{I}}\big|_i$ is

$$\Delta P_{\mathrm{I}}\big|_i = P_{\mathrm{E}}\big|_i - P_{\mathrm{I}}\big|_i \tag{16.12}$$

Finally, we approximate the force increment as

$$\Delta \underline{P}_{\mathrm{I}}\big|_i = K_{\mathrm{t}}\big|_i \Delta \underline{U}\big|_i \tag{16.13}$$

where K_{t} represents a "tangent" stiffness matrix for the structure. The incremental equilibrium equation takes the form

$$K_{\mathrm{t}}\big|_i \;\; \Delta \underline{U}\big|_i = P_{\mathrm{E}}\big|_i - P_{\mathrm{I}}\big|_i \tag{16.14}$$

One cycles on (16.14) until successive value of $\Delta \underline{U}$ agree to a specified tolerance. Instability occurs where K_{t} is singular.

One determines ΔP_{I} by operating on (16.9). For example, noting

$$\begin{aligned} \Delta P_1 &= \int \Phi_{1,xx}^{\mathrm{T}}\, \Delta M\, dx \\ \Delta M &= 0 \qquad \text{for} \quad \chi > \chi_r \\ \Delta M &= k_t\, \Delta\chi \quad \text{for} \quad \chi_y < \chi < \chi_r \\ \Delta M &= k_E\, \Delta\chi \quad \text{for} \quad \chi < \chi_y \\ \Delta\chi &= \Phi_{1,xx}\, \Delta U_1 + \Phi_{2,xx}\, \Delta U_2 \end{aligned} \tag{16.15}$$

leads to

$$\Delta P_1 = \left[\int \Phi_{1,xx}^{\mathrm{T}} k^* \Phi_{1,xx} \mathrm{d}x\right] \Delta U_1 + \left[\int \Phi_{2,xx}^{\mathrm{T}} k^* \Phi_{2,xx} \mathrm{d}x\right] \Delta U_2$$

where $k^* = k_E, k_t,$ or 0 depending on the value of χ.

One applies the external load in increments and cycles at each load level. This approach generates the complete nonlinear load-displacement response history for the structure, i.e., it determines the order and location of plastic hinges as the load is increased, and the final limit state. Most commercial structural software have this capability. The following examples illustrate the nonlinear analysis process.

Example 16.6

Given: The portal frame defined in Fig. E16.6a. Consider the gravity loading w to be constant. The lateral load P is due to seismic excitation. Material is steel, $\sigma_{\mathrm{y}} = 50$ ksi, and $w = 4.17$ kip/ft.

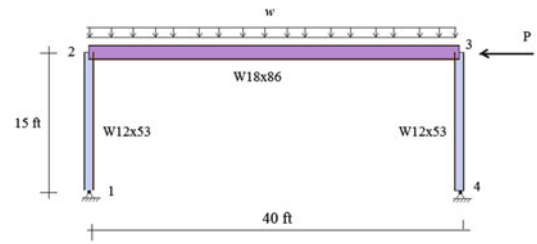

Fig. E16.6a

Determine: The inelastic response of the frame and the limiting values of P and S_a.

Solution: The analysis of gravity loaded frames subjected to lateral loading is referred to as a pushover analysis. One common application is to estimate the capacity of a frame for seismic excitation. One applies the lateral loading in increments and generates the nonlinear response up to the onset of instability. The pushover analysis was done using computer software [3] and the result is plotted in Fig. E16.6b.

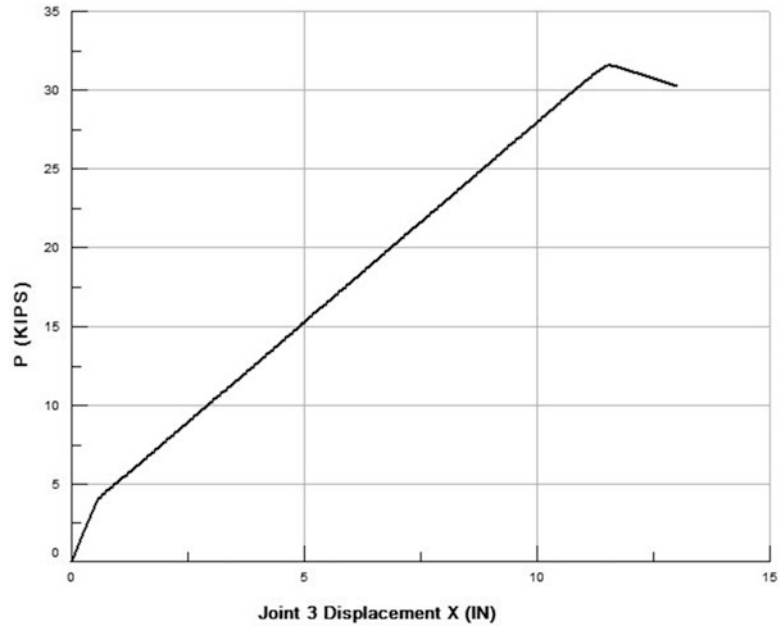

Fig. E16.6b Pushover results, P vs. joint displacement

Using the materials presented in Sect. 14.2.2, one can relate P to the spectral acceleration. For a single degree of freedom system, this relationship reduces to

$$P \approx mS_a$$

where m is the lumped mass and S_a is the spectral acceleration.

$$P_{max} = 32\,\text{kip}$$

$$m = \frac{4.17(40)}{g} = \frac{166.8}{g}$$

$$S_a = \frac{P_{max}}{m} = 0.19g$$

Example 16.7

Given: The three-story frame defined in Fig. E16.7a. Consider the gravity floor loading to be constant. The lateral load is due to seismic excitation. The material is steel, $\sigma_y = 50\,\text{ksi}$, and the gravity floor load =0.75 kip/ft

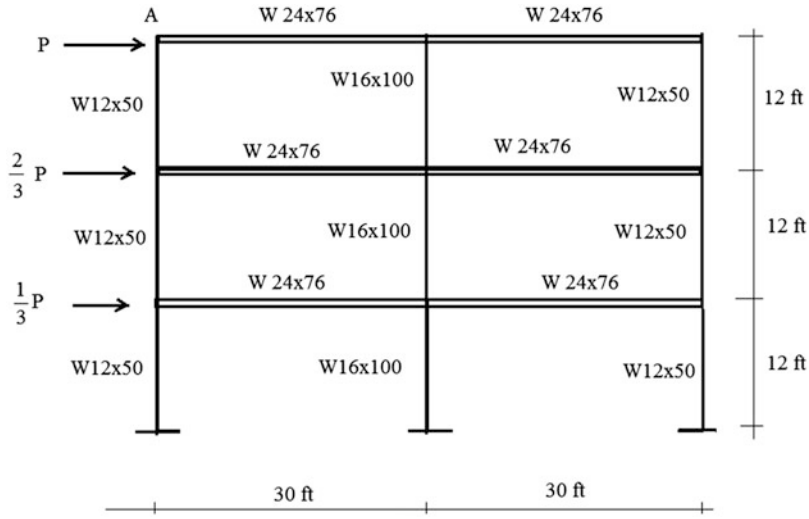

Fig. E16.7a

Determine: The lateral displacement of point A versus P and the limiting value of S_a.
Solution: We use Equation (14.9) specialized for this structure

$$P = m\Gamma S_a$$

where m is the mass of a typical floor, $m = \dfrac{0.75(60)}{g} = \dfrac{45}{g}$

Noting (14.7), $\Gamma = \dfrac{9}{7}$ for this frame.

One applies the lateral loading in increments and generates the nonlinear response up to the onset of instability. The pushover analysis was done using computer software [3] and the result is plotted in Fig. E16.7b.

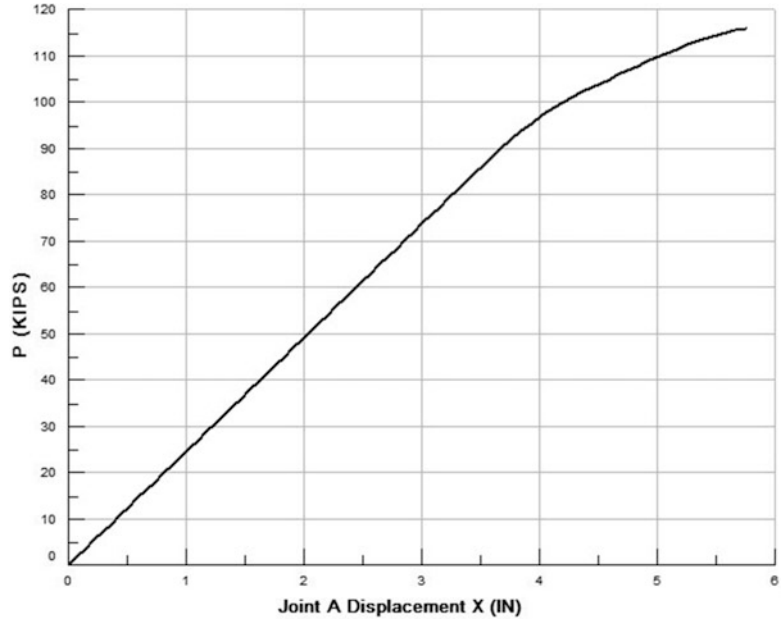

Fig. E16.7b Pushover results, P vs. joint displacement

Then

$$S_{\mathrm{a}} = \frac{P_{\max}}{m\Gamma} = \frac{115}{\left(\frac{45}{g}\right)\left(\frac{9}{7}\right)} = 1.98g$$

16.5 Summary

16.5.1 Objectives

- Describe the different regions of the stress–strain behavior of structural steels and concrete: elastic; inelastic.
- Extend the moment–curvature relationships to the inelastic range and estimate the moment capacity of a beam subjected to inelastic bending.
- Present analysis procedures for determining the maximum external load that a structure can support using: (a) hand calculation methods and (b) finite element computation-based methods. This general topic is called "Limit Analysis."
- Include some examples which illustrate how analysis is applied to simple rigid frames.

16.6 Problems

Problem 16.1 Determine the load capacity.

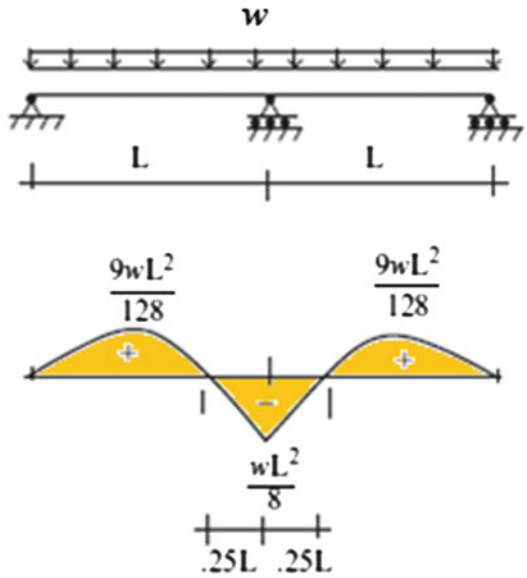

Problem 16.2 Determine the load capacity.

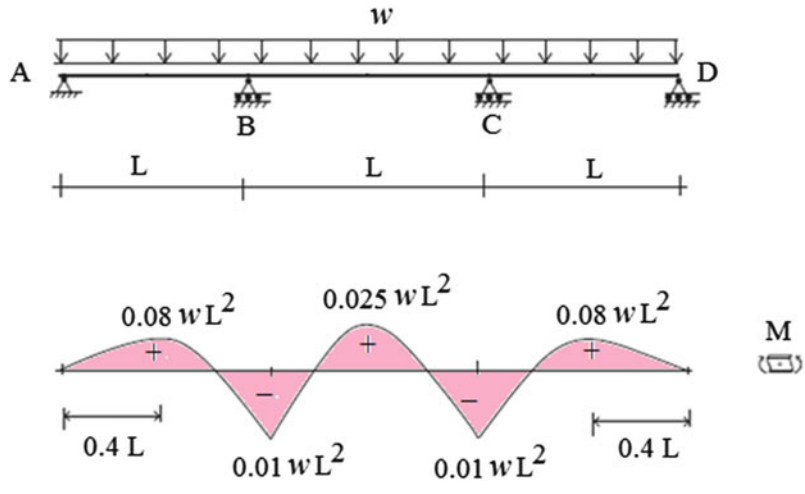

Problem 16.3 Determine w_{max} as a function of α.

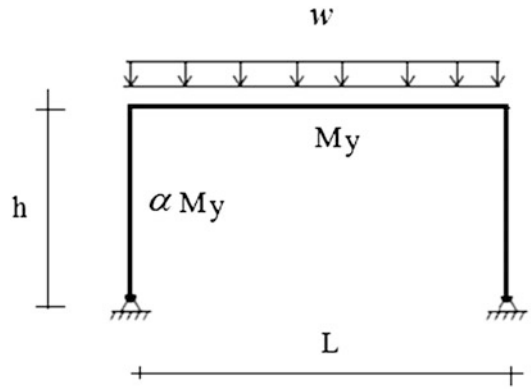

Problem 16.4 Determine an expression for P_{max}.

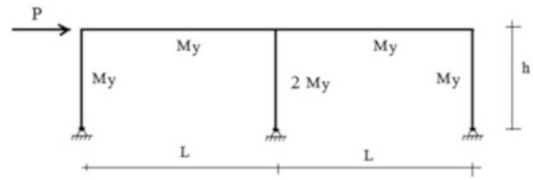

Problem 16.5 Generate the plot of P vs. u for the frame shown. Consider w as a dead loading. Assume $\alpha = 1.2$.

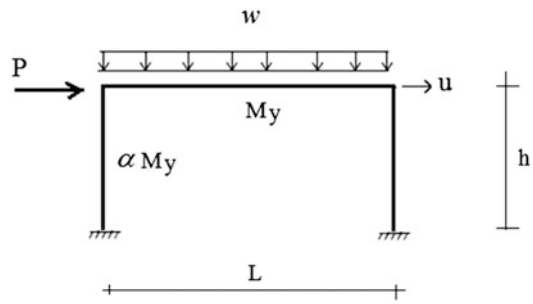

Problem 16.6 Using computer software, generate the plot of u_A vs. P, and estimate P_{max}. Take $w = 1.5$ kip/ft, $h = 12$ ft, and $L = 30$ ft. The material is steel, $\sigma_y = 50$ ksi. The exterior columns are W16 × 89, the interior columns are aW16 × 100, and all the beams are W24 × 131.

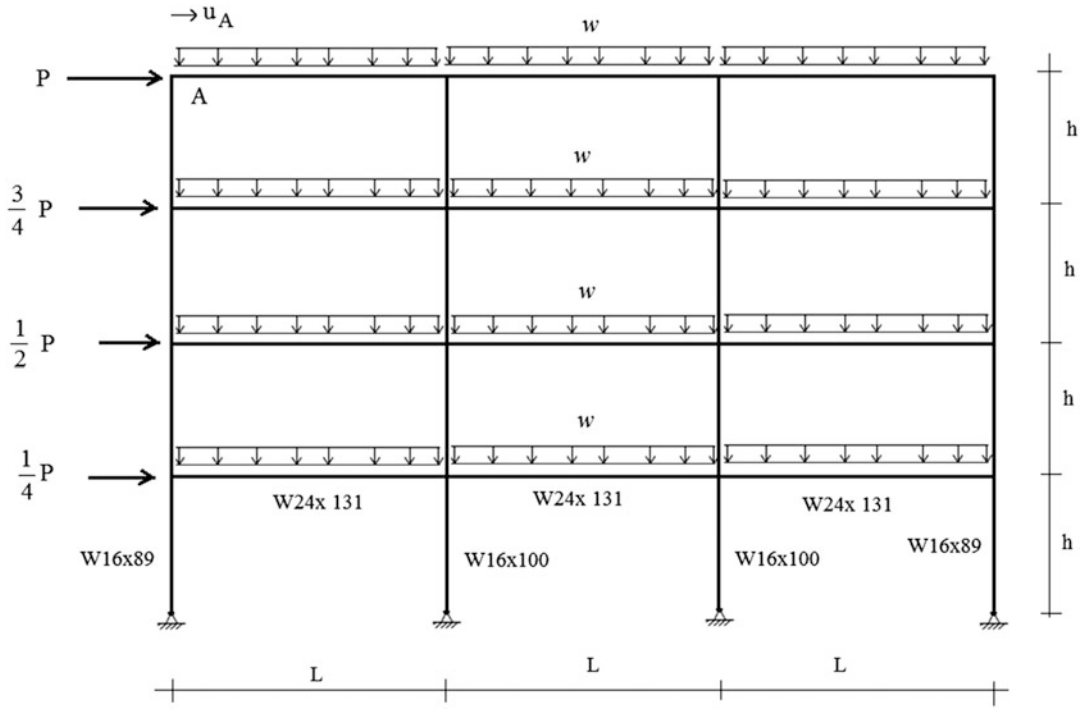

References

1. Nilson AH. Design of concrete structures. 14th ed. New York: McGraw Hill; 2013.
2. Bathe KJ. Finite element procedures. 1st ed. Prentice Hall: Upper Saddle River; 1995.
3. GTSTRUDL. Intergraph Corporation PP&M, Norcross, GA, USA.